

# Numerical weather prediction for the Antarctic & the Arctic

David H. Bromwich<sup>1,2</sup>, Jordan G. Powers<sup>3</sup>,  
Aaron B. Wilson<sup>1</sup>, Karen Pon<sup>1,2</sup>, and Julien P. Nicolas<sup>1,2</sup>

<sup>1</sup>Byrd Polar Research Center, Ohio State University, Columbus, Ohio, USA

<sup>2</sup>Atmospheric Sciences Program, Department of Geography,  
Ohio State University, Columbus, Ohio, USA

<sup>3</sup>National Center for Atmospheric Research, Boulder, Colorado, USA

## 1. Introduction

The Polar Meteorology Group (PMG) of the Byrd Polar Research Center at Ohio State University (OSU) has conducted numerical weather prediction (NWP) of the Antarctic and Arctic using regional models for more than a decade. Specifically, the PMG has focused on the development of the Weather Research and Forecasting (WRF) model (Skamarock et al. 2008) for use in polar regions (Polar WRF) including testing this model over the Greenland Ice Sheet (Hines et al. 2008), Arctic Ocean (Bromwich et al. 2009), Arctic land (Hines et al. 2011), and Antarctica (Bromwich et al. 2013). Optimizations focus primarily on the sea ice cover of the polar oceans and the land surface model for ice sheets and for seasonally snow covered land. Here, the application of Polar WRF for weather forecasting in the Antarctic is outlined and followed by a forecast performance analysis in the mid and high latitudes of the Northern Hemisphere that focuses on the atmospheric hydrologic variables.

## 2. Antarctic Mesoscale Prediction System (AMPS)

The AMPS effort (Powers et al. 2003, 2012) is a project of the National Center for Atmospheric Research and OSU to develop and maintain an experimental, real-time, high-resolution NWP capability for the United States Antarctic Program (USAP). The original core objective was to establish a mesoscale weather modeling system covering Antarctica to serve the USAP forecasters employed by the Space and Naval Warfare Center (SPAWAR). Originally, they were stationed at McMurdo Station on Ross Island, the main United States base in Antarctica, but now much of the forecasting is done remotely from Charleston, South Carolina. The impetus for AMPS was the Antarctic Weather Forecasting Workshop of May 2000, which identified key weaknesses in Antarctic NWP for the USAP (Bromwich and Cassano 2001). The AMPS effort was proposed to address these, namely: to establish a robust NWP system for the forecasters serving the USAP; to provide model products tailored to the needs of the forecasters; to improve physical process parameterizations for the Antarctic; to perform model verification; and to stimulate collaboration among Antarctic weather forecasters, modelers, and researchers.

AMPS forecasting started in late 2000, and the first version was tested in the 2000–2001 field season. AMPS currently provides twice-daily forecasts covering the Southern Ocean and Antarctica, with higher-resolution grids over key areas of the continent (e.g., the McMurdo region). The forecasts are primarily provided through the main AMPS web page: <http://www.mmm.ucar.edu/rt/amps>. Although their priority is for support of the USAP and SPAWAR, the forecasts are also used by many foreign nations (listed below). The initial motivations for AMPS have been served, and the system has evolved to provide forecasts of much higher resolution (to 1.1 km), longer duration (to 120 hr), and greater variety than first envisioned.

Figure 1 presents AMPS's array of regular forecast grids. The primary setup now has domains of 30-km, 10-km, 3.33-km, and 1.11-km horizontal spacing. All of the grids within the outermost domain are two-way interactive. Figure 1a shows the current Southern Ocean and Antarctic domains, which have 30-km and 10-km spacing. Figure 1b shows the 3.3-km Ross Ice Shelf/South Pole and 3.3-km Antarctic Peninsula grids within the 10-km continental domain. The highest-resolution 1.1-km grid covers the critical Ross Island region (Fig. 1c), and Fig. 2 reveals how the resolution can better capture the complex flows there. Seen in better detail are the katabatic outflows of Byrd Glacier to the south of Minna Bluff and Reeves Glacier at Terra Nova Bay to the north of McMurdo. Also seen is a lee vortex to the north of Ross Island, forced by the strong southerly flow around it. All the grid sizes were enhanced to these scales (from 45 km, 15 km, 5 km, and 1.67 km) in early 2013. The forecast model used by AMPS is Polar WRF. The initial and lateral boundary conditions for AMPS are derived from the National Centers for Environment Prediction (NCEP) Global Forecasting System with regional data assimilation of conventional and satellite observations using WRFDA (the WRF data assimilation package; see for example, Huang et al. 2009) to enhance the model's initial state.

Occasionally AMPS serves Antarctic emergency operations. Prominent examples are the 2001 medical evacuation of Dr. Ronald Shemenski from the South Pole well after the closing of the station for winter operations (Monaghan et al. 2003) and the 2002 marine rescue of the ice-bound ship *Magdalena Oldendorff* (Powers et al. 2003). Over the years AMPS has also provided forecast information for medical evacuations from the South Pole and McMurdo, with the AMPS team working with SPAWAR during these episodes.

Beyond its support for the USAP, the AMPS effort has been prominent in the organization of the annual Antarctic Meteorological Observation, Modeling, and Forecasting (AMOMF) Workshop. This workshop brings together the Antarctic forecasting, observation, and research communities to discuss Antarctic meteorology and related logistics and science. Since 2006 the AMOMF Workshop has fostered this interaction with international participation. Most recently, in 2013 the University of Wisconsin– Madison hosted the 8<sup>th</sup> AMOMF Workshop (June) in Madison, WI, and the 9<sup>th</sup> will be held in Charleston in 2014. The international use of AMPS has also been promoted in the workshops. Foreign nations using AMPS include: Italy, UK, Australia, Germany, Chile, South Africa, Argentina, China, and New Zealand, and collectively, the DROMLAN (Droning Maud land Air Network) Group (Germany, South Africa, UK, Norway, Sweden, Finland, India, Russia, Belgium, and Japan). The siting of the AMOMF Workshop in Rome, Italy in 2007, in Hobart, Australia in 2011, and Cambridge, UK in 2015 demonstrates the strengthened international ties of the Antarctic meteorological community, in part from AMPS-related efforts.

## **2.1 AMPS and forecasting of the Prydz Bay Low**

The Ingrid Christensen coast of East Antarctica, along the eastern side of Prydz Bay, is home to the bases of Davis (Australia), Progress II (Russia), Zhongshan (China) and Bharati (India). It generally experiences relatively benign weather conditions. It is not subject to a strong katabatic regime, nor is it frequently affected by synoptic-scale cyclones. One of the main causes of poor weather conditions is a mesoscale feature, the Prydz Bay Low. This feature is examined here to illustrate some of the successes and limitations of the current AMPS forecasts.

The Prydz Bay Low is a shallow, relatively short-lived circulation which usually forms in the absence of strong synoptic influences. It brings extensive low cloud and precipitation to the Ingrid Christensen coast. It can hamper station operations, in particular aviation safety, making it a significant forecasting problem.

Figures 3 to 7 show an example from 22 January 2013. Figures 3 to 6 show the 30-hour AMPS forecast valid for 06UTC 22 January 2013 of, respectively, surface wind; sea level pressure and precipitation; relative humidity (at 1 km AGL); and cloud base. Figure 7 shows the 0415UTC 22 January 2013 visible satellite image from MODIS Terra.

Forecasting of the Prydz Bay Low is difficult as it is too small to be resolved by global models and very little research has thus far been undertaken to identify its development mechanisms. The winds around this circulation are light, with no significant difference in strength to the broader environmental flow (Fig. 3). Similarly the pressure gradient is weak compared with the surrounding environment (Fig. 4).

AMPS is the only system to reliably forecast this phenomenon however it is not an unqualified success. The surface (10 m) wind (Fig. 3) and 1-km relative humidity (Fig. 5) fields are usually the most reliable for predicting the formation of the Prydz Bay Low. Although the low is associated with extensive low cloud and precipitation, the cloud base field (Fig. 6) typically underestimates the actual extent of low cloud which occurs and the precipitation field (Fig. 4) is unreliable. Comparison of the low level humidity field (Fig. 5) with the satellite image (Fig. 7) shows that it is more accurately reflects the actual low cloud.

### **3. Forecasting with Polar WRF in the Arctic**

Modifications to WRF including those to the physics of snow surfaces, the addition of fractional sea-ice and varying sea-ice depth, and time-varying snow cover on sea ice have all improved the model's performance. In preparation for the Arctic System Reanalysis (ASR) (Bromwich et al. 2010), two additional studies of the pan-Arctic atmosphere have been performed utilizing a number of improvements from previous experiments that demonstrate the success of Polar WRF in producing accurate short-term forecasts of state variables and the hydrologic cycle over the annual cycle throughout the Arctic (Wilson et al. 2011, 2012). These studies highlight the need for continued improvement in the representation of clouds and their effects on downward surface radiation.

#### **3.1 State Variables**

Wilson et al. (2011) show that state variables from Polar WRF short-term forecasts compare well with a variety of observational data, re-iterating results from earlier experiments on smaller domains throughout the Arctic (Hines et al. 2008; Bromwich et al 2009; Hines et al. 2011). A spatial comparison with ERA-Interim Reanalysis (ERA-I) (Dee et al. 2011) shows near-surface air temperature patterns agree well, with Polar WRF providing a higher degree of detail in areas of complex terrain. For analysis purposes, stations along and north of 60°N are referred to as "polar" and those south of this are referred to as "mid-latitude". Three-hourly biases in near-surface air temperatures from Polar WRF compared to observations from the National Climatic Data Center (NCDC) are cold throughout most of the domain, but the biases are small (-1.1°C) and correlations are high (0.80) giving confidence that Polar WRF accurately predicts 2-m temperature. Analysis of 2-m dewpoint temperatures follows the 2-m temperature patterns in the polar region but shows a warm bias in the mid-latitudes

(0.3°C) which is attributed to excessive evaporation over land particularly during summer. Polar WRF predicted differences in surface pressure are small as well (-1.1 hPa) with high correlations ( $\geq 0.98$ ) at most sites. Near-surface wind speeds are well predicted ( $0.7 \text{ m s}^{-1}$ ) even though the correlations suffer from the coarse model resolution (60 km) and inadequate depiction of local wind effects. Finally, upper level temperatures and wind speeds over the polar region are well captured by Polar WRF, with temperature biases generally less than  $1^\circ\text{C}$  and wind speed biases  $\pm 1 \text{ m s}^{-1}$ .

### 3.2 Precipitation

Representing a comprehensive evaluation of the pan-Arctic hydrologic cycle and an extension over earlier Polar WRF studies, Wilson et al. (2012) analyze precipitation, clouds, and surface radiation. Besides the annual precipitation (sum of all three-hourly model convective and non-convective precipitation) in Polar WRF comparing well with ERA-I, a monthly analysis of Polar WRF compared to observations from the Global Historical Climate Network (GHCN) version 2 (Peterson and Vose 1997) and the Adjusted Historical Canadian Climate Data (AHCCD, Mekis and Hogg 1999) was conducted. Figure 8 shows monthly Polar WRF and observed precipitation totals, biases, and Polar WRF convective and non-convective precipitation. Clearly evident is a warm/cool season discrepancy in model behavior. During the winter and early spring in the mid-latitudes (Fig. 8a), precipitation biases are small (e.g., February (+0.5%) and March (1.7%)). From late spring into summer, large positive precipitation biases occur, especially in June (+35.2%), July (+16.2%), and August (+15.2%). In the polar region (Fig. 8b), all months reflect negative precipitation biases (-20.1% to -5.5%), except during July (+11.0%) when the greatest contribution to model precipitation is convective. It is during this month that the most convective contribution to model precipitation is evident, and the model behaves in this region as it does in the mid-latitudes during the entire summer. This supports the idea that excessive convection during warm months in Polar WRF leads to a surplus of precipitation. This excessive precipitation has been linked to an abundance of evaporation in Polar WRF over land surfaces causing too much low level moisture available for convective processes during this season. This is further supported by the fact that during the cooler months, the main contribution of precipitation in Polar WRF is non-convective, leading to primarily negative precipitation biases in both the mid-latitudes and polar region.

### 3.3 Clouds

Figure 9 shows Polar WRF cloud fraction (CF) for July 2007. Here the cloud fraction is based on the integrated cloud optical depth which is computed using the cloud liquid water path and cloud ice water path along with Arctic-appropriate weighting coefficients for each type (see Wilson et al. 2012). Two methods are used for Polar WRF CF: a monthly average (Fig. 9a) and a cloud frequency (CFreq) (Fig. 9b) which is defined by the ratio between the 3-h forecasts when the model CF exceeds zero to the total number of forecasts (248) for July 2007. Derived cloud products are used for comparison, specifically the National Aeronautics and Space Administration's Moderate Resolution Imaging Spectroradiometer (MODIS) aboard Terra and Aqua satellites as well as the co-located CloudSat radar and Cloud and Aerosol Lidar with Orthogonal Polarization (CALIOP) aboard the Cloud-Aerosol Lidar and Infrared Pathfinder Satellite Observations (CALIPSO) satellite. Recent improvements to cloud-detection schemes in MODIS are described by Frey et al. (2008) and Ackerman et al. (2008). CloudSat radar and CALIPSO lidar have been combined to produce gridded monthly CF (Kay and Gettelman 2009). Polar WRF (Fig. 9a) is consistent with the satellite products

(Figs. 9c and 9d), showing greater CF in areas of higher terrain (most likely associated with orographic lift and enhanced windward precipitation) and within the North Pacific and North Atlantic storm tracks (less than depicted by MODIS). Kay et al. (2008) note that the western Arctic was abnormally cloud free during the summer of 2007 due to a strong Beaufort Sea high. However, CF over land in the western Arctic (0.1-0.2) in this simulation is lower than CF analyzed by Hines et al. (2011). In fact, CF over the entire Arctic Ocean remains much lower than observed by MODIS, suggesting an underrepresentation of Arctic stratus clouds in the model. As a result of counting any CF greater than zero towards the CFreq, Fig. 9b represents an ample opportunity for clouds in the model. This method increases CF throughout the entire domain, but Polar WRF is still lower than both MODIS and CloudSat/CALIPSO. Therefore, even the most conservative approach to estimating clouds still reveals a deficit in cloud cover in the model for July, which results in a large anomalous diurnal cycle of 2-m temperature (Wilson et al. 2011), excessive incident shortwave radiation, and a deficit in downwelling longwave (LW) radiation at the surface.

### 3.4 Surface Longwave Radiation

Finally, radiation measurements from a number of sources have been collected for analysis with Polar WRF (see Wilson et al. 2012, Table 1). Figure 10 shows scatter plots of 3-hr model LW vs. observed LW radiation for July 2007 for the mid-latitude (six stations) and polar region (three stations) under varying conditions of model cloud species availability in order to classify events ((a) cloud water and/or cloud ice available, (b) no cloud water or cloud ice, (c) cloud water available regardless of cloud-ice availability, and (d) cloud ice only). The mid-latitudes show strong correlations between Polar WRF and observations for all cases considered, with only subtle differences. When cloud water and/or cloud ice is present in the vertical column (Fig. 10a), the negative model LW biases are the result of not enough cloud cover in the model. Under clear sky conditions when no cloud water or cloud ice is present (Fig. 10b), the model agrees better with observations. The performance of model LW is greatly impacted by the presence of cloud water as biases are strongly negative during this case (Fig. 10c). This is opposite to what is expected as liquid water within the clouds should lead to an increase in downwelling LW. For the polar region, the correlations suffer tremendously because the performance of model LW radiation in this region is less than ideal. All cases show negative LW radiation biases, with an insensitivity between cloud water/cloud ice conditions and clear sky. Sensitivity tests of various LW schemes in Polar WRF have led to little improvement in these results. Hines et al. (2011) conclude that the lack of clouds throughout the domain appears to be an issue with subgrid-scale non-precipitating clouds. The LW biases in the polar region shown here, along with the sensitivity of the selection of microphysics schemes over land versus water and the excessive mixing of water vapor in the vertical inhibiting moisture availability for low clouds (Hines et al. 2011), all strongly encourage continued improvements to the representation of clouds (cover and thickness), cloud radiative effects due to cloud water, and moisture fluxes into the boundary layer in Polar WRF.

## 4. Conclusion

Polar WRF forecasts the surface and tropospheric state variables with high skill in both polar regions on the multi-day time scale. More problematic are deficiencies in forecast low clouds and their impact on the downwelling radiation fluxes at the surface with again similar behavior in the Antarctic and Arctic. This is an area of future efforts to improve Polar WRF forecast behavior.

## Acknowledgments

The work summarized here was supported by grants from NSF Division of Polar Programs and NASA.

## References

- Ackerman, S. A., R. E. Holz, R. Frey, E. W. Eloranta, B. C. Maddux, and M. McGill, 2008: Cloud detection with MODIS. Part II: Validation. *J. Atmos. Ocean Tech.*, **25**, 1073-1086, doi:10.1175/2007JTECHA1053.1.
- Bromwich, D. H., and J. J. Cassano, 2001: Meeting Summary: Antarctic Weather Forecasting Workshop. *Bull. Amer. Meteor. Soc.*, **82**, 1409-1413.
- Bromwich, D. H., K. M. Hines, and L.-S. Bai, 2009: Development and testing of Polar WRF: 2. Arctic Ocean. *J. Geophys. Res.*, **114**, D08122, doi:10.1029/2008JD010300.
- Bromwich, D. H., Y.-H. Kuo, M. Serreze, J. Walsh, L.-S. Bai, M. Barlage, K. M. Hines, and A. Slater, 2010: Arctic System Reanalysis: Call for community involvement. *Eos, Trans. Amer. Geophys. Union*, **91(2)**, 13-14.
- Bromwich, D. H., F. O. Otieno, K. M. Hines, K. W. Manning, and E. Shilo, 2013: Comprehensive evaluation of polar weather research and forecasting performance in the Antarctic. *J. Geophys. Res.*, **118**, 274-292, doi: 10.1029/2012JD018139.
- Dee, D., and Coauthors, 2011: The ERA-Interim reanalysis: Configuration and performance of the data assimilation system. *Q. J. R. Meteor. Soc.*, **137(656)**, 553-597, doi:10.1002/qj.828.
- Frey, R. A., S. A. Ackerman, Y. Liu, K. I. Strabala, H. Zhang, J. R. Key, and X. Wang, 2008: Cloud detection with MODIS. Part I: Improvements in the MODIS cloud mask for collection 5. *J. Atmos. Ocean Tech.*, **25**, 1057-1072, doi:10.1175/2008JTECHA1052.1.
- Hines, K. M., and D. H. Bromwich, 2008: Development and testing of Polar WRF Part I: Greenland ice sheet meteorology. *Mon. Wea. Rev.*, **136**, 1971-1989, doi:10.1175/2007MWR2112.1.
- Hines, K. M., D. H. Bromwich, L.-S. Bai, M. Barlage, and A. G. Slater, 2011: Development and testing of Polar WRF: Part III. Arctic land. *J. Clim.*, **24**, 26-48.
- Huang, X.-Y., and Co-Authors, 2009: Four-dimensional variational data assimilation for WRF: Formulation and preliminary results. *Mon. Wea. Rev.*, **137**, 299-314.
- Kay, J. E., and A. Gettelman, 2009: Cloud influence on and response to seasonal Arctic sea ice loss. *J. Geophys. Res.*, **114**, D18204, doi:10.1029/2009JD011773.
- Kay, J. E., T. L'Ecuyer, A. Gettelman, G. Stephens, and C. O'Dell, 2008: The contribution of cloud and radiation anomalies to the 2007 Arctic sea ice extent minimum. *Geophys. Res. Lett.*, **35**, L08503, doi:10.1029/2008GL033451.

Mekis, È, and W. D. Hogg, 1999: Rehabilitation and analysis of Canadian daily precipitation time series. *Atmosphere-Ocean*, **37(1)**, 53-85.

Monaghan, A. J., D. H. Bromwich, H. Wei, A. M. Cayette, J. G. Powers, Y.-H. Kuo, and M. Lazzara, 2003: Performance of weather forecast models in the rescue of Dr. Ronald Shemenski from South Pole in April 2001. *Wea. Forecasting*, **18**, 142-160, doi: 10.1175/1520-0434(2003)018<0142:POWFMI>2.0.CO;2.

Peterson, T. C., and R. S. Vose, 1997: GHCN V2-Global Historical Climatology Network, 1697-present, National Oceanic and Atmospheric Administration, National Climate Data Center, Asheville, North Carolina, USA, (Available online at <http://lwf.ncdc.noaa.gov/oa/climate/research/ghcn/ghcngrid.html>), Accessed January 25, 2010.

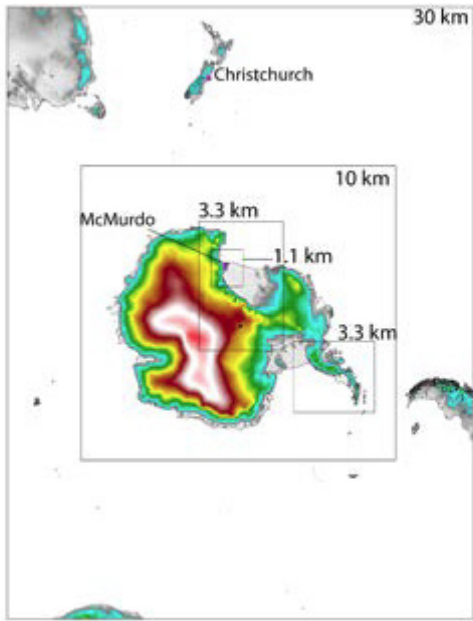
Powers, J. G., A. J. Monaghan, A. M. Cayette, D.H. Bromwich, Y.-H. Kuo, and K. W. Manning, 2003: Real-time mesoscale modeling over Antarctica: The Antarctic Mesoscale Prediction System (AMPS). *Bull. Amer. Meteor. Soc.*, **84**, 1533-1545, doi: 10.1175/BAMS-84-11-1533.

Powers, J., K. W. Manning, D. H. Bromwich, J. J. Cassano, and A. M. Cayette, 2012: A decade of Antarctic science support through AMPS. *Bull. Amer. Meteor. Soc.*, **93**, 1699-1712, doi: 10.1175/BAMS-D-11-00186.1.

Skamarock, W. C., J. B. Klemp, J. Dudhia, D. Gill, D. Barker, M. Dudhia, X.-Y. Huang, W. Wang, and J. G. Powers, 2008: A description of the Advanced Research WRF Version 3, NCAR Tech. Note, NCAR/TN-475+STR, 113 pp.

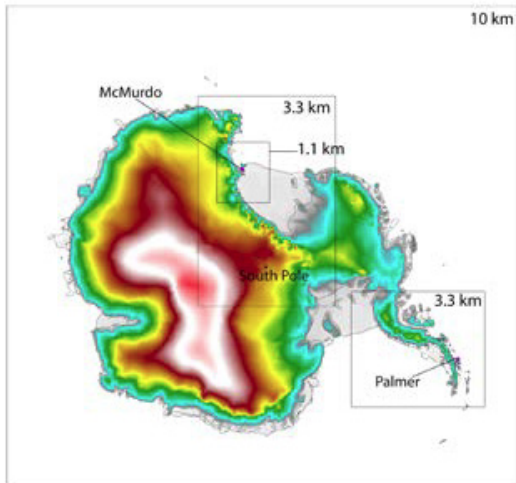
Wilson, A. B., D. H. Bromwich, and K. M. Hines, 2011: Evaluation of Polar WRF Forecasts on the Arctic System Reanalysis Domain, Surface and Upper Air Analysis. *J. Geophys. Res.*, **116**, D11112, doi:10.1029/2010JD015013.

Wilson, A. B., D. H. Bromwich, and K. M. Hines, 2012: Evaluation of Polar WRF forecasts on the Arctic System Reanalysis domain. 2. Atmospheric hydrologic cycle. *J. Geophys. Res.*, **117**, D04107, doi: 10.1029/2011JD016765.



(a)

(b)



(c)

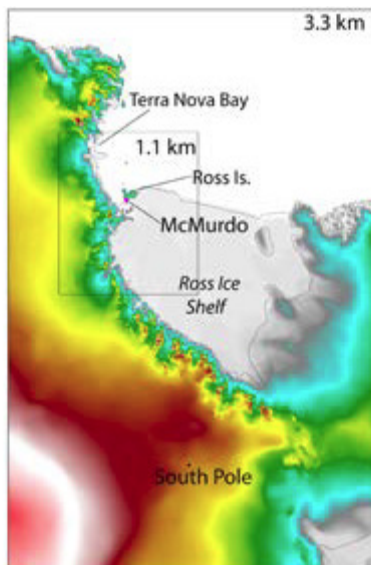


**Figure 1.** AMPS forecast domains. (a) 30-km and 10-km grids. (b) 10-km Antarctic and 3.3-km Ross Sea and Antarctic Peninsula grids. (c) 3.3-km Ross Sea and 1.1-km Ross Island grids.

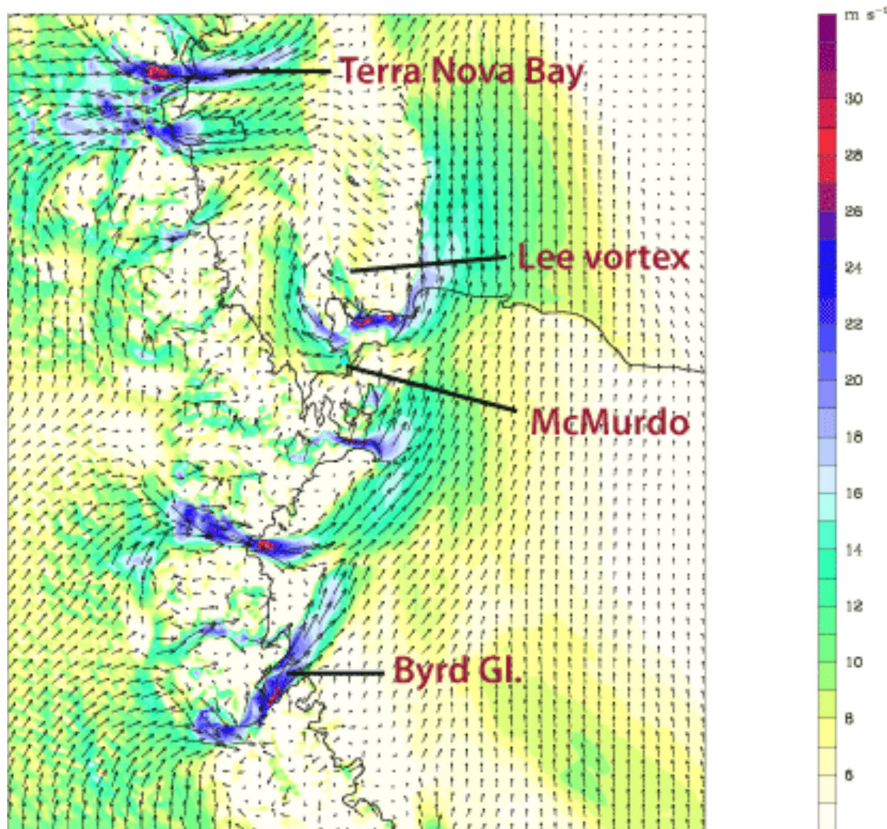


**Figure 2.** 1.1-km AMPS domain for the Ross Island area. 12-hr forecast valid at 1200 UTC 17 June 2013 shown. 10-m winds ( $\text{ms}^{-1}$ ) shaded, scale to right. Surface wind vectors shown.

**Figure 3.** 10-m wind field from AMPS forecast for 06UTC 22 January 2013.

AMPS 10-km WRF -- Davis-Mawson Window  
Fcst. 30 h  
Total precip. in past 3 h  
Sea-level pressure

Init. 00 UTC Mon 21 Jan 13  
Valid. 06 UTC Tue 22 Jan 13

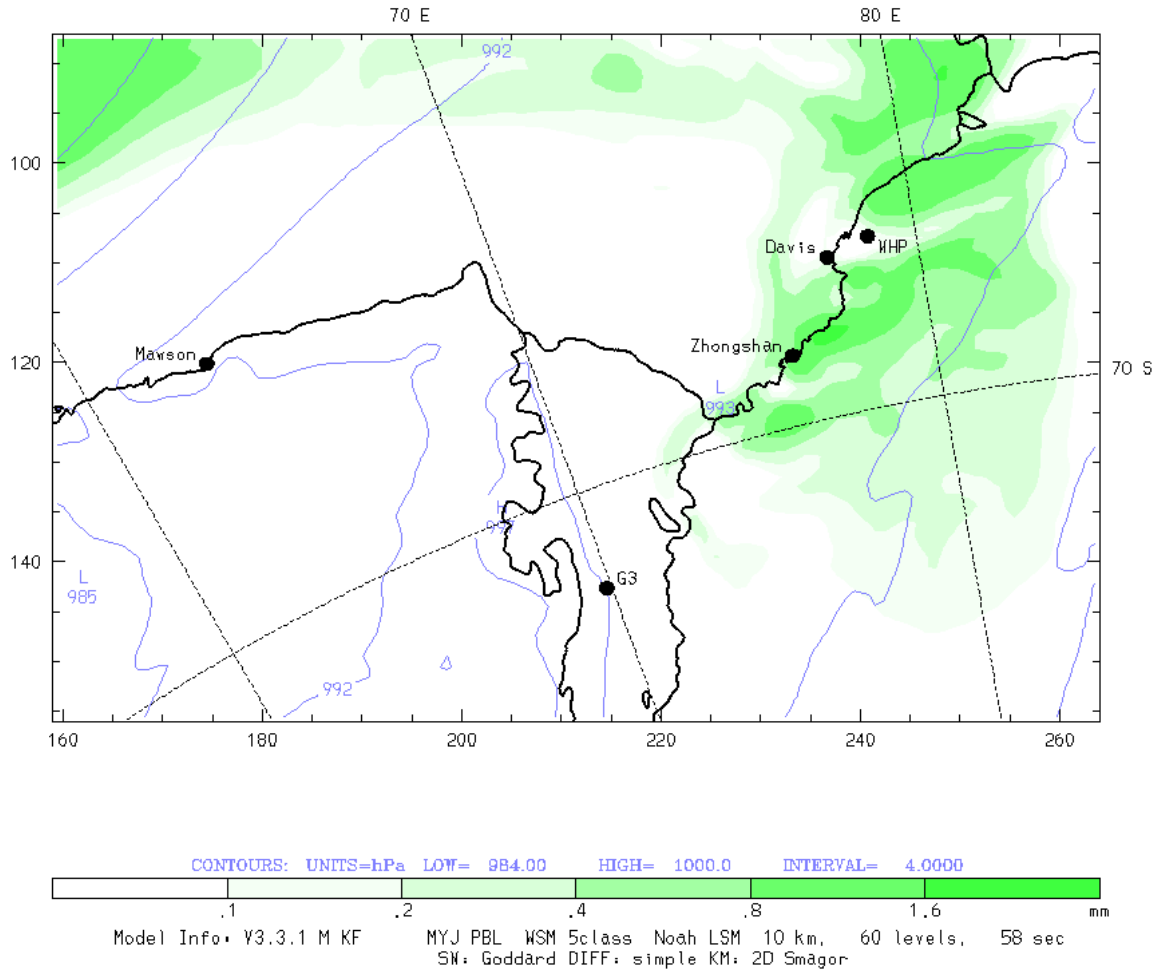


**Figure 4.** Sea level pressure and precipitation field from AMPS forecast for 06UTC 22 January 2013.

**Figure 5.** 1-km relative humidity and wind field from AMPS forecast for 06UTC 22 January 2013.

**Figure 6.** Cloud base field from AMPS forecast for 06UTC 22 January 2013.

**Figure 7.** Visible satellite image from MODIS Terra for 0415UTC on 22 January 2013

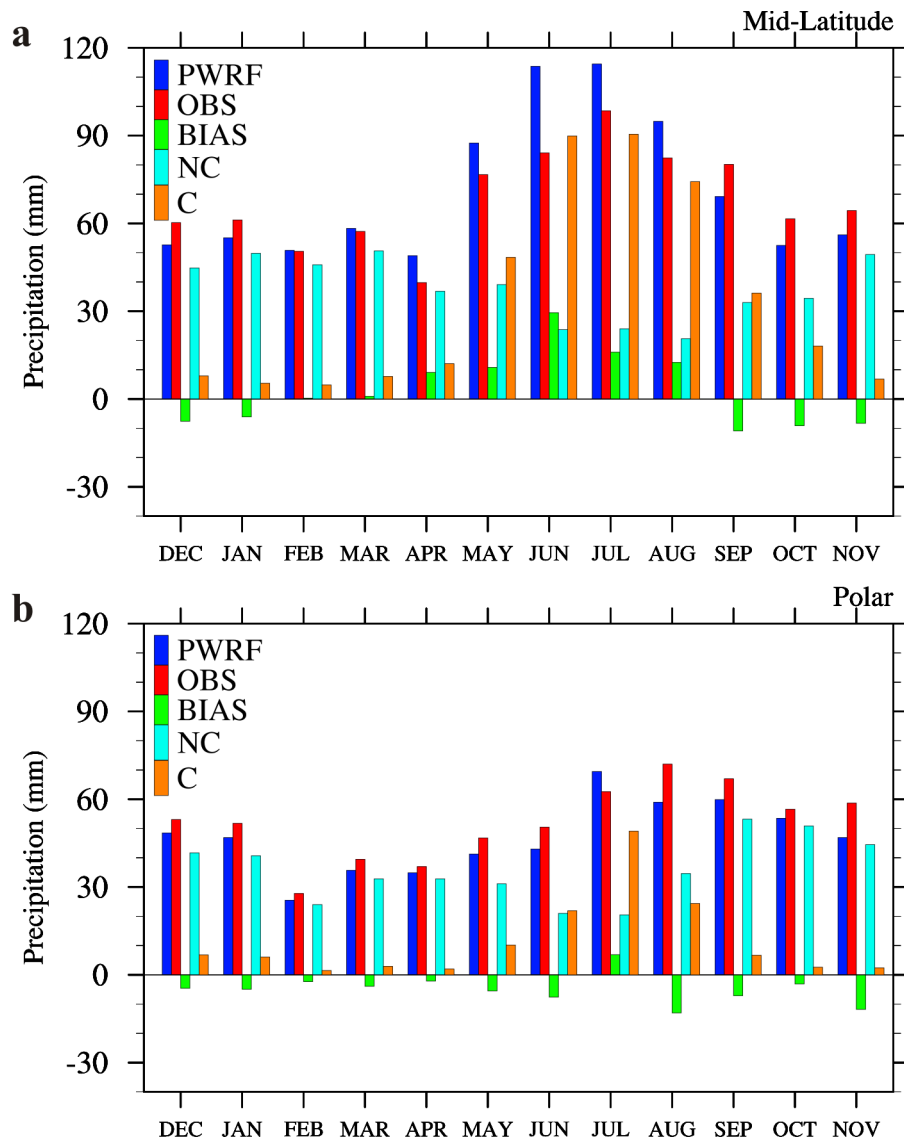


**Figure 8.** Monthly precipitation totals (mm) for Polar WRF and observations for (a) mid-latitude and (b) polar region. The bias (green) is the model (blue) minus observed precipitation (red). Non-convective (NC, light-blue) and convective (C, orange) components of the model precipitation are also provided. From Wilson et al. (2012).

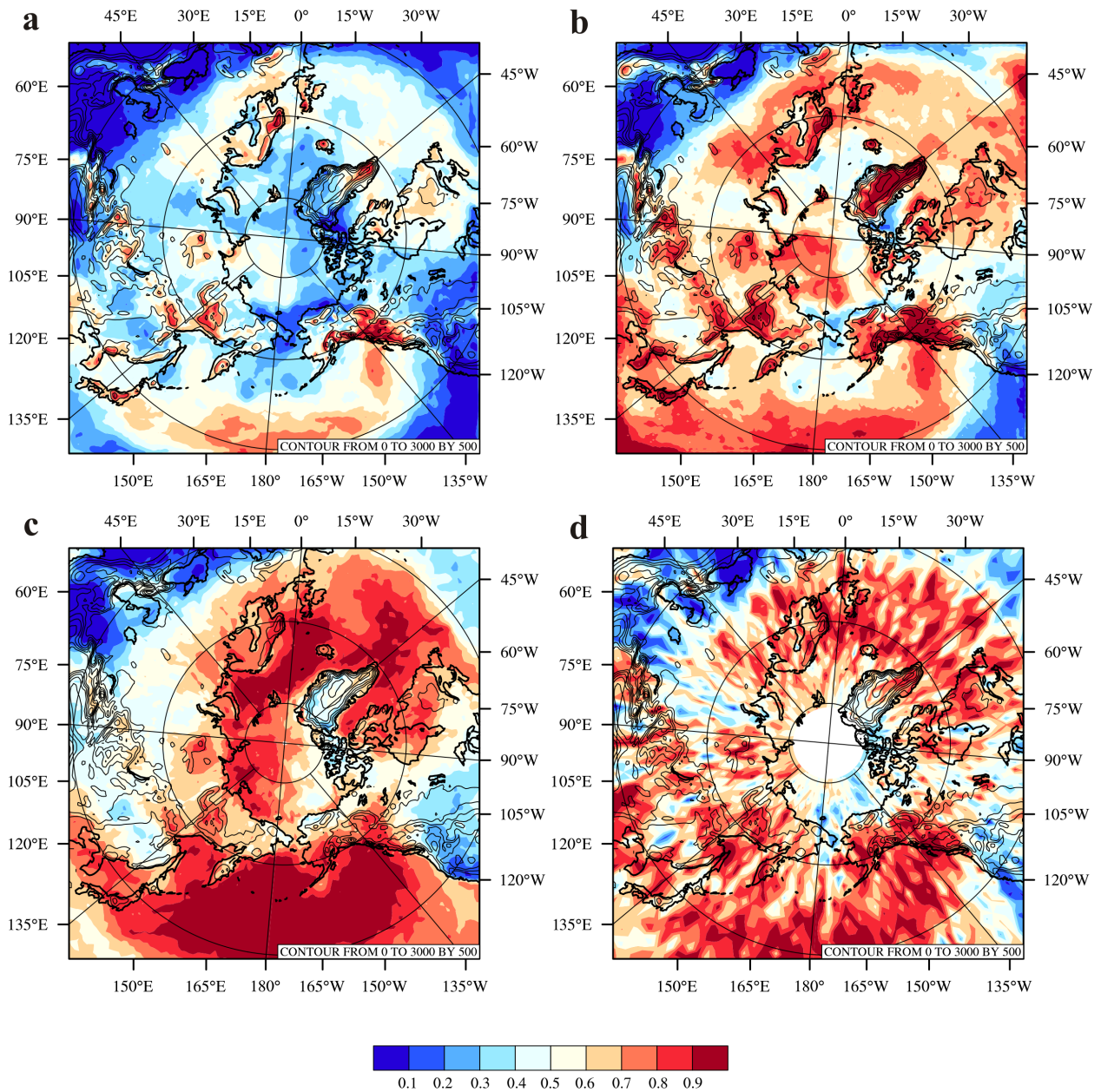


**Figure 9.** July 2007 (a) Polar WRF monthly average CF based on vertically integrated cloud water and cloud ice, (b) Polar WRF CFreq defined by the ratio of the 3-h forecasts where the model CF exceeds zero to the total number of forecasts for July 2007, (c) MODIS CF based on the cloud mask estimates of cloudy  $1 \text{ km}^2$  pixels averaged within a  $5 \times 5 \text{ km}$  grid cell on a  $1^\circ \times 1^\circ$  grid, and (d) CloudSat/CALIPSO based on the merged cloud mask product on a  $2^\circ \times 2^\circ$  grid. Terrain elevation is contoured to 3000 m in 500 m increments. From Wilson et al. (2012).

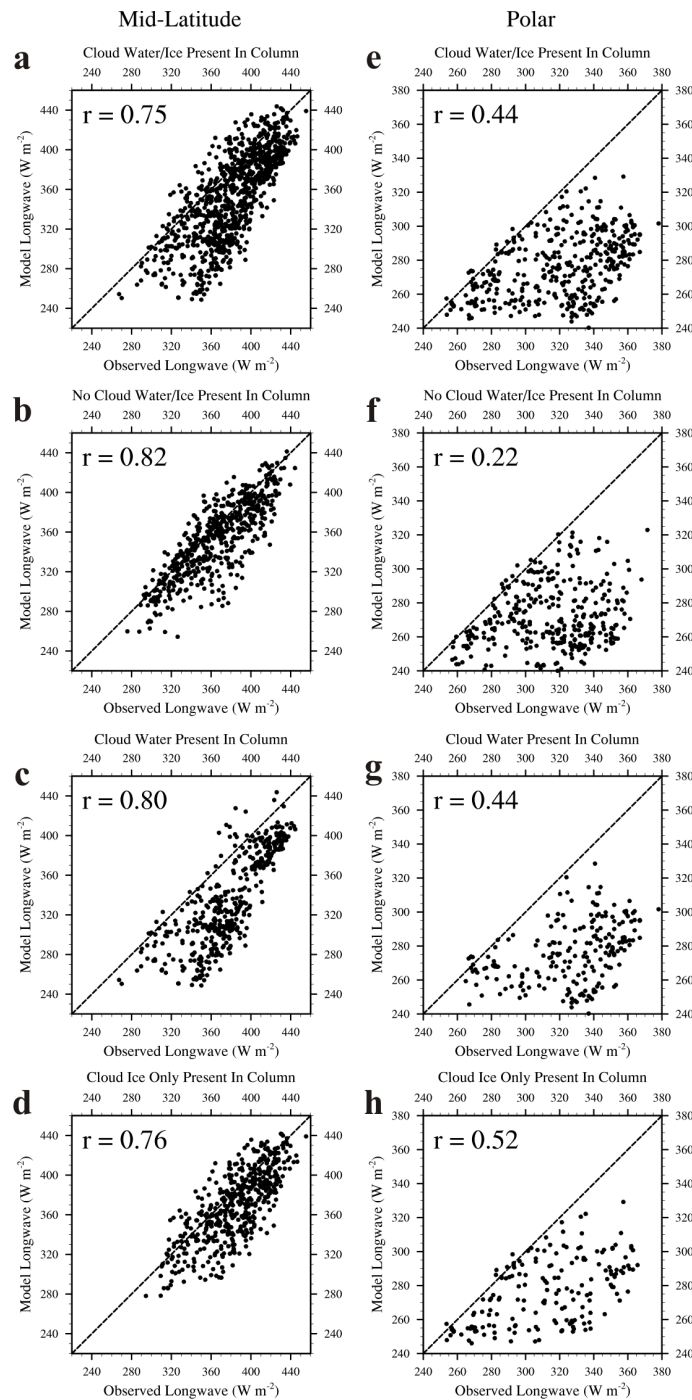


**Figure 10.** Scatter plots of model vs. observed LW radiation for July 2007 under the following model conditions: (a) and (e) cloud water and/or cloud ice present in the vertical column, (b) and (f) no cloud water or cloud ice in the vertical column, (c) and (g) cloud water in the vertical column regardless of cloud ice, and (d) and (h) cloud ice only in the vertical column for mid-latitude region (left; six stations combined) and polar region (right; three stations combined). From Wilson et al. (2012).